Inorganic Chemistry

Article

pubs.acs.org/IC

Chemical and Structural Evolution in the Th−SeO_3^{2-}/SeO_4^{2-} System: from Simple Selenites to Cluster-Based Selenate Compounds

Bin Xiao,[†,‡] Eike Langer,[†,‡] Jakob Dellen,[†] Hartmut Schlenz,[†] Dirk Bosbach,[†] Evgeny V. Suleimanov,[§] and Evgeny V. Alekseev*[,†,‡]

[†]Institute of Energy and Climate Research (IEK-6), Forschungszentrum Jülich GmbH, 52428 Jülich, Germany

[‡]Institut für Kristallographie, RWTH Aachen University, 52066 Aachen, Germany

[§]Department of Chemistry, Lobachevsky State University of Nizhny Novgorod, 603950 Nizhny Novgorod, Russia

Supporting Information

ABSTRACT: While extensive success has been gained in the structural chemistry of the U−Se system, the synthesis and characterization of Th-based Se structures are widely unexplored. Here, four new Th−Se compounds, α-$Th(SeO_3)_2$, β-$Th(SeO_3)_2$, $Th(Se_2O_5)_2$, and $Th_3O_2(OH)_2(SeO_4)_3$, have been obtained from mild hydrothermal or low-temperature (180−220 °C) flux conditions and were subsequently structurally and spectroscopically characterized. The crystal structures of α-$Th(SeO_3)_2$ and β-$Th(SeO_3)_2$ are based on ThO_8 and SeO_3 polyhedra, respectively, featuring a three-dimensional (3D) network with selenite anions filling in the Th channels along the *a* axis. $Th(Se_2O_5)_2$ is a 3D framework composed of isolated ThO_8 polyhedra interconnected by $[Se_2O_5]^{2-}$ dimers. $Th_3O_2(OH)_2(SeO_4)_3$ is also a 3D framework constructed by octahedral hexathorium clusters $[Th_6(\mu_3\text{-}O)_4(\mu_3\text{-}OH)_4]^{12+}$, which are interlinked by selenate groups SeO_4^{2-}. The positions of the vibrational modes associated with both $Se^{IV}O_3^{2-}$ and $Se^{VI}O_4^{2-}$ units, respectively, were determined for four compounds, and the Raman spectra of α- and β-$Th(SeO_3)_2$ are compared and discussed in detail.

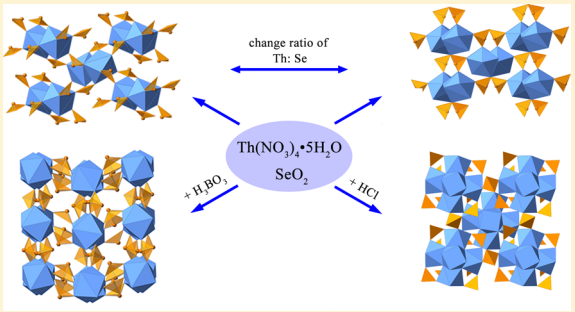

1. INTRODUCTION

The chemical behavior of actinide compounds has attracted intensive concerns for the last decades owing to their significant role in the safe handling of radioactive waste and disposal of spent nuclear fuel.[1,2] Th, unlike most of the early actinides possessing various oxidation states, is practically solely stable in tetravalent state Th^{IV}. This condition makes Th a practical analogue for studying the more radioactive and toxic Np^{IV} and Pu^{IV}.[3] From a structural point of view, Th can achieve considerably large coordination numbers that vary from 6 to 15, resulting in fascinating topological geometries. $[Th(H_2O)_{10}]Br_4$, as an outstanding representative encompassing 10 coordinating water molecules for one Th site, has become the only homoleptic aqua complex among all tetravalent ions to date.[4] Another noticeable example is $[ThB_5O_6(OH)_6][B(OH)_2]\cdot 2.5H_2O$ (NDTB-1), which is built from a cationic framework presenting a remarkable anion-exchange capability that is especially highlighted by the selective removal of TcO_4^- from nuclear waste streams.[5−7] In an aqueous solution, Th^{IV} tends to hydrolyze and to construct a wide diversity of $Th(OH)_n^{4-n}$ hydroxide complexes, the olation or oxolation of which can further result in the formation of polynuclear compounds.[8,9] Numerous polynuclear thorium hydroxide species have already been isolated, including dimers such as $Th_2(OH)_2^{6+}$, $Th_2(OH)_3^{5+}$, and $Th_2(OH)_4^{4+}$, respectively, tetramers such as $Th_4(OH)_8^{8+}$ and $Th_4(OH)_{12}^{4+}$, pentamer $Th_5(OH)_{12}^{8+}$, and hexamers such as $Th_6(OH)_{14}^{10+}$ and $Th_6(OH)_{15}^{9+}$.[10] The largest Th oligomer up to now, to the best of our knowledge, is the decanuclear $[Th_{10}F_{16}O_8(NH_3)_{32}]^{8+}$ formed in $[Th_{10}F_{16}O_8(NH_3)_{32}](NO_3)_8\cdot 19.6NH_3$.[11] These polynuclear compounds, in conjunction with the aggregates and colloids of actinides, have already gathered extensive attention because of the role of transporting and migrating radionuclides to the environment.[12,13]

^{79}Se is one of the prominent long-lived fission products that form within the nuclear fuel cycle.[14] The predominant forms of Se are either selenite $Se^{IV}O_3^{2-}$ or selenate $Se^{VI}O_4^{2-}$ in oxosalt compounds. Owing to the existence of the stereochemically active lone-pair electrons in Se^{4+}, the SeO_3^{2-} ions can act as the so-called structure-directing agents to yield a relatively large number of structure types with, consequently, promising physical properties such as second-harmonic generation, piezoelectricity, ferroelectricity, and magnetic properties.[15−17] In recent years, one could witness the robust growth and an exuberant development related to the synthesis and characterization of U^{VI}−Se compounds, which exhibit diverse structural units from common sheet to the unique $[(UO_2)_3(SeO_4)_5]^{4-}$ nanotubes.[18,19]

Received: January 20, 2015
Published: February 26, 2015

DOI: 10.1021/acs.inorgchem.5b00133
Inorg. Chem. 2015, 54, 3022−3030

Table 1. Crystallographic Data of α-$Th(SeO_3)_2$, β-$Th(SeO_3)_2$, $Th(Se_2O_5)_2$, and $Th_3O_2(OH)_2(SeO_4)_3$

	α-$Th(SeO_3)_2$	β-$Th(SeO_3)_2$	$Th(Se_2O_5)_2$	$Th_3O_2(OH)_2(SeO_4)_3$
mass	485.96	485.96	707.88	1189.00
space group	$P2_1/n$	$Pna2_1$	$Pbca$	$I4/m$
a (Å)	7.1816(7)	7.2226(9)	12.4048(7)	11.1252(3)
b (Å)	10.7842(12)	11.0808(18)	11.8424(6)	11.1252(3)
c (Å)	7.4290(8)	6.6427(7)	12.9828(11)	10.819(1)
β (deg)	107.58(1)	90	90	90
V (Å^3)	548.5(1)	531.63(12)	1907.2(2)	1339.07(14)
Z	4	4	4	4
λ (Å)	0.71073	0.71073	0.71073	0.71073
$F(000)$	824.0	824.0	2448.0	2000.0
μ (cm^{-1})	40.413	41.694	30.942	41.477
ρ_{calcd} (g cm^{-3})	5.885	6.072	4.931	5.898
R1(F) for $F_o^2 > 2\sigma(F_o^2)$[a]	0.0293	0.0445	0.0241	0.0393
wR2(F_o^2)[b]	0.0656	0.1131	0.0557	0.1040

[a] $R1(F) = \sum||F_o| - |F_c||/\sum|F_o|$. [b] $wR2(F_o^2) = [\sum w(F_o^2 - F_c^2)^2/\sum w(F_o^4)]^{1/2}$.

The Se systems containing Th^{IV}, as well as the other low-valent actinides such as Np^{IV} and Pu^{IV}, have already been known for more than half a century.[20] The first synthesized Th−Se compounds are the octahydrate $Th(SeO_3)_2{\cdot}8H_2O$ and monohydrate $Th(SeO_3)_2{\cdot}H_2O$ produced by the precipitation method, but there is a lack of crystallographic studies that support or confirm these proposed compounds.[20] The first reported crystal structure of the Th−Se system is $Th(SeO_3)(SeO_4)$ by Sullens et al. in 2006. It is an interesting mixed anion compound consisting of both SeO_3^{2-} trigonal-pyramidal and SeO_4^{2-} tetrahedral oxoanions.[21] Following this, recently, by investigating the condensation of Th^{IV} under aqueous conditions, Knope et al. obtained and reported four novel selenate compounds containing an octanuclear $[Th_8O_4(OH)_8]^{16+}$ core.[22] However, compared to the U^{VI} counterparts, studies on the Th−Se compounds are still barely explored and are quite scarce. Detailed knowledge of the crystallographic features of the actinide compounds is the essential precondition for establishing a structure−property relationship in order to model complex processes in nuclear waste disposal sites. This is a scientific basis for the safe handling of nuclear waste. Going along this line, we started a systematical exploration on the reaction of thorium(IV) salts with selenium oxide under mild hydrothermal and low-temperature (180−220 °C) flux conditions, and such efforts resulted in the isolation of four new compounds with Se in different valence states: α-$Th(Se^{IV}O_3)_2$, β-$Th(Se^{4+}O_3)_2$, $Th(Se^{IV}{}_2O_5)_2$, and $Th_3Se^{VI}{}_3O_{14}(OH)_2$.

2. EXPERIMENTAL SECTION

Crystal Growth. *α- and β-$Th(SeO_3)_2$.* The synthesis processes for both polymorphs were quite similar. The differences were the ratio and amount of initial reactants. Our first attempt was to obtain Th−Se compounds containing alkaline cations. Thus, the sodium nitrate was also included for sample synthesis. For α-$Th(SeO_3)_2$, 100 mg of $Th(NO_3)_4{\cdot}5H_2O$ (0.175 mmol), 58.4 mg of SeO_2 (0.526 mmol), 74.5 mg of $NaNO_3$ (0.877 mmol), and 4 mL of H_2O were weighed and added. This results in a Th/Se/Na ratio of 1:3:5. For β-$Th(SeO_3)_2$, 100 mg of $Th(NO_3)_4{\cdot}5H_2O$ (0.175 mmol), 19.5 mg of SeO_2 (0.175 mmol), 44.7 mg of $NaNO_3$ (0.526 mmol), and 4 mL of H_2O were weighed and added. This results in a Th/Se/Na ratio of 1:1:3. The mixtures were filled in 23 mL autoclaves and placed inside a program-controlled furnace (MEMMERT). They were heated at a rate of 100 °C/h to 220 °C and held there for roughly 48 h. The furnace was then cooled to room temperature with a cooling rate of 4.2 °C/h. Apparently, the Na was not incorporated into both structures. The α-$Th(SeO_3)_2$ crystals were colorless and shaped as long prisms, while for β-$Th(SeO_3)_2$, the shape however was more compact and did not show any elongation into a specific direction.

$Th(Se_2O_5)_2$ was synthesized by the low-temperature flux method. A total of 100 mg of $Th(NO_3)_4{\cdot}(H_2O)_5$ (0.175 mmol), 97.3 mg of SeO_2 (0.877 mmol), and 216.9 mg of H_3BO_3 (3.5 mmol) were weighed and added. This results in a Th/Se/B ratio of 1:5:20. A total of 100 μL of water was added. The temperature profile, however, was slightly different compared to the syntheses of α- and β-$Th(SeO_3)_2$, respectively. The filled autoclave was placed inside the furnace at room temperature and was heated at a rate of 100 °C/h for 2 h to 220 °C. After a holding time of 48 h, the furnace was cooled in two steps. First the temperature was gradually reduced at a rate of 1.75 °C/h to 150 °C and then to room temperature within 3 h. Apparently, B played the part of a flux during the crystal growth process and was not incorporated into the structure.

$Th_3O_2(OH)_2(SeO_4)_3$ was obtained by using hydrothermal synthesis. An initial ratio of the reactants of 1:1 for Th/Se resulted in the reported structure. That is to say, 100 mg of $Th(NO_3)_4{\cdot}(H_2O)_5$ (0.175 mmol), 19.5 mg of SeO_2 (0.175 mmol), and 0.2 mL of 1 M HCl (0.2 mmol) were weighed and added, and the autoclave was loaded with an additional small amount of water (2 mL). The furnace containing the autoclave was heated up from room temperature to 220 °C in 2 h, keeping the temperature constant for about 48 h. Cooling to room temperature was also done in about 48 h at a constant cooling rate of 4.2 °C/h. The product of this synthesis resulted in, typical for Th^{IV}, colorless crystals.

Crystal Structure Studies. The as-obtained Th−Se crystals were selected for data collection. The crystals were mounted on glass fibers and optically aligned on an Agilent diffractometer (SuperNova, Dual Source). Data collection was done using a monochromatic Mo Kα tube, which has an incident wavelength of 0.71073 Å and runs at 50 kV and 0.8 mA providing a beam size of approximately 30 μm. The unit-cell dimensions for these crystals were refined using least-squares techniques against the positions of all measured reflections. More than a hemisphere of data were collected for each crystal, and the three-dimensional (3D) data were reduced and filtered for statistical outliers using the standard *CrysAlis^{Pro}* program. Data were corrected for Lorentz, polarization, absorption, and background effects. The crystal structure determination and refinement were carried out using the *SHELXL-97* program.[23] The data and crystallographic information are given in Table 1. The structures were solved by direct methods and refined to R1 = 0.029 for α-$Th(SeO_3)_2$, R1 = 0.045 for β-$Th(SeO_3)_2$, R1 = 0.024 for $Th(Se_2O_5)_2$, and R1 = 0.039 for $Th_3O_2(OH)_2(SeO_4)_3$, respectively.

Scanning Electron Microscopy (SEM)/Energy-Dispersive Spectroscopy (EDS). SEM images and EDS data were collected using a FEI Quanta 200F environment scanning electron microscope.

DOI: 10.1021/acs.inorgchem.5b00133
Inorg. Chem. 2015, 54, 3022−3030

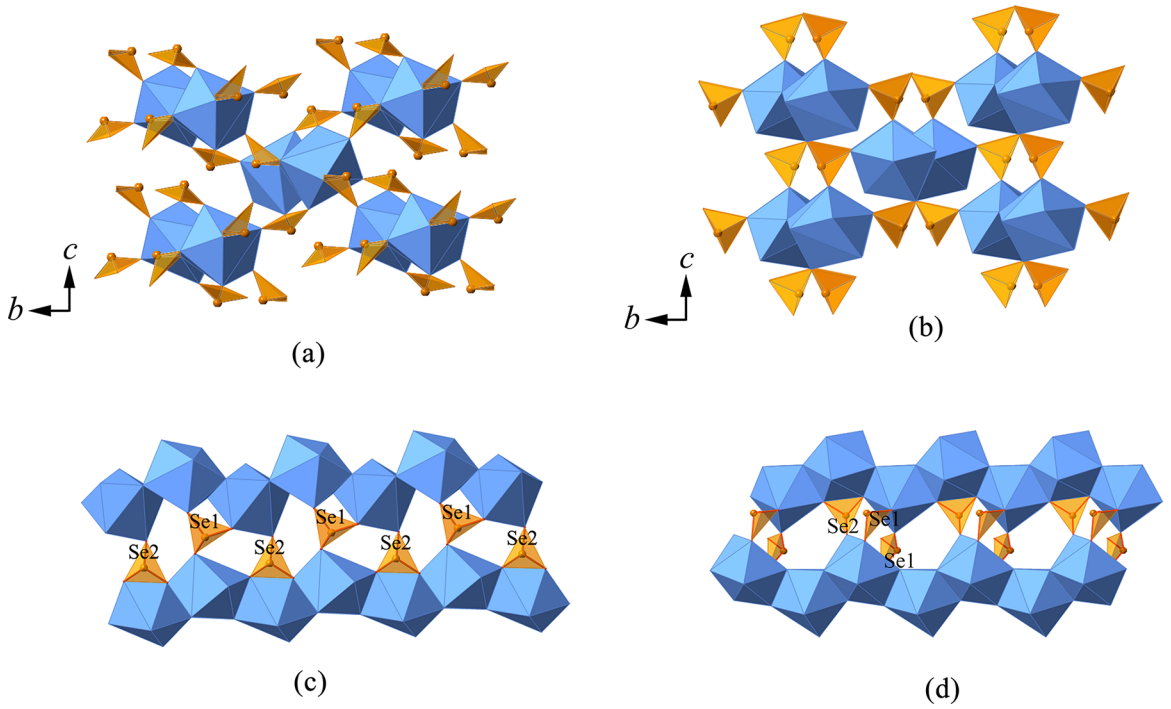

Figure 1. Polyhedral representation of the structures of two polymorphs of $Th(SeO_3)_2$. (a) 3D framework in α-$Th(SeO_3)_2$. (b) 3D framework in β-$Th(SeO_3)_2$. (c) Linkage manners for Se sites in α-$Th(SeO_3)_2$. (d) Linkage manners for Se sites in β-$Th(SeO_3)_2$. Blue and orange polyhedra represent ThO_8 and SeO_3, respectively.

The EDS results are in good agreement with the proposed chemical compositions for all four Th−Se compounds.

Raman Spectroscopy. Using a Peltier-cooled multichannel CCD detector, the unpolarized Raman spectra were recorded with a Horiba LabRAM HR spectrometer. All of the samples were in the form of single crystals. An objective with 50× magnification was linked to the spectrometer, allowing analysis of samples as small as 2 μm diameter. The incident radiation was produced by a He−Ne laser at a power of 17 mW (λ = 632.81 nm). The focal length of the spectrometer was 800 mm, and a 1800 grooves/mm grating was used. The spectral resolution was around 1 cm^{-1} with a slit of 100 μm. The Raman spectroscopic investigation for all samples was executed at room temperature in the range of 100−3000 cm^{-1}. Except for $Th_3O_2(OH)_2(SeO_4)_3$, which reveals Raman shifts of around 3000 cm^{-1} derived from the hydroxyl units, the spectra for all other Th−Se compounds do not show any peaks exceeding 1000 cm^{-1}. Hence, the presented spectra for these compounds will only be exhibited in the range from 100 to 1000 cm^{-1}.

Bond Valence Analysis. Bond valence sums (BVSs) for all atom positions in the four Th−Se compounds were calculated. The bond valence parameters for Th^{IV}−O, Se^{IV}−O, and Se^{VI}−O are used according to Brese and O'Keefee.[24] The BVSs for all atoms are consistent with their expected formal valences.

3. RESULTS AND DISCUSSION

Syntheses. All of the titled Th−Se compounds have been obtained at temperatures of around 220 °C. Isolation of α- and β-$Th(SeO_3)_2$ from hydrothermal conditions is very likely to be driven by stoichiometry. The reagent ratio of the starting materials controls the formation of these two compounds. α-$Th(SeO_3)_2$ is more favored at a low Th/Se ratio, and β-$Th(SeO_3)_2$ can be present when the amount of Se is increased. Compared to α- and β-$Th(SeO_3)_2$, $Th(Se_2O_5)_2$ obtained using boric acid as the flux is characterized by a very high Th/Se ratio. This method has been proven to be an effective way to synthesize novel actinide borates in the past few years.[25−30] Borate acid, which does not include into the structure of $Th(Se_2O_5)_2$, serves the role of reaction medium; its presence, however, without a doubt plays an important role in the process of crystallization. In addition to this, we also found that the thorium−selenium borates can be formed by modifying the stoichiometry ratio of the starting materials, but this will be part of another publication. Up to now, most of the polynuclear Th complexes are synthesized via a slow precipitation method with organic acids as reaction media.[31] To the best of our knowledge, $Th_3O_2(OH)_2(SeO_4)_3$ is the first inorganic hexanuclear Th material prepared under hydrothermal conditions. It is worth noting that hydrothermal conditions lead to a Th coordination number equal to 8 in $Th_3O_2(OH)_2(SeO_4)_3$, which is different from the 9-fold coordination environment in the previous reported hexanuclear Th clusters.[31]

***α*-Th(SeO$_3$)$_2$.** The α-$Th(SeO_3)_2$ polymorph, crystallizing in the monoclinic system with space group $P2_1/n$, contains one independent Th position and two Se sites, as shown in Figure 1a. It adopts the $CeSe_2O_6$[32] structure type, which has also been found in the compounds $CeTe_2O_6$,[33,34] $ThTe_2O_6$,[34] $PuTe_2O_6$,[35] and $PuSe_2O_6$,[36] respectively. The Th atom is coordinated by eight O atoms with an average Th−O bond distance of 2.42 Å, which fits well with other Th compounds.[37,38] In order to determine the polyhedral geometry of Th, a shape-measuring algorithm was carried out.[39] The output of the algorithm is a value S, which is the minimal variance of all dihedral angles along all edges. The lower this value, the higher is the resemblance to the ideal polyhedron. The obtained S values [$S(D_{2d})$ = 18.7°, $S(C_{2v})$ = 18.3°, and $S(D_{4d})$ = 19.5°] demonstrate the bicapped trigonal-prismatic geometry of the Th polyhedra. The coordination type as well as determined bond angles are comparable to those of other inorganic Th^{IV} compounds.[40,41] Se1 and Se2 are both

DOI: 10.1021/acs.inorgchem.5b00133
Inorg. Chem. 2015, 54, 3022−3030

coordinated by three O atoms, respectively, in a trigonal-pyramidal geometry with the Se atom situated at the apical vertex, exhibiting an asymmetric coordination environment that arises from the stereoactive nonbonded electron pairs. Adjacent ThO_8 polyhedra are edge-connected with two O atoms, forming corrugated chains extending along the [100] direction. The chains are further linked together to construct the 3D framework with the help of trigonal-pyramidal SeO_3 groups. The $Se1O_3$ polyhedra share all three O atoms with Th chains in a corner-sharing configuration, that is, two O atoms with two ThO_8 from a single chain and the third O atom with another ThO_8 from a different chain. However, the $Se2O_3$ groups share a common edge with a ThO_8 polyhedron from one chain and a corner with another chain (Figure 1c). The different connection geometries result in different bond length configurations for Se1 and Se2 despite the fact that both are very similar in their average lengths (1.70 Å). The Se2 polyhedra are more distorted [from 1.673(6) to 1.719(6) Å] compared to Se1 polyhedra [from 1.698(6) to 1.703(6) Å]. The related angles in Se2 also show an abnormal behavior, with one notably smaller angle for the edge-sharing O atoms [91.7(3)°]. The average of 98.3° for Se2 is slightly smaller than 101.9° for Se1 but agrees well with other reported values for compounds containing Se^{IV} lone-pair electrons.[42−44]

β-$Th(SeO_3)_2$. The β-$Th(SeO_3)_2$ polymorph adopts an orthorhombic crystal system with the $Pna2_1$ space group. The structure of this polymorph is presented in Figure 1b. Similar to α-$Th(SeO_3)_2$, it consists of one symmetrically independent Th position and two Se positions. The Th atom is also coordinated by eight O atoms with an average bond distance of 2.44 Å. Shape-measure calculations for the Th polyhedron result in a distorted trigonal dodecahedron. The Th polyhedra share one common edge with one another, leading to chains propagating along the [100] direction. Notably, there is a broad range of distances for the Th−O bonds from 2.32(2) to 2.77(1) Å. The average Se−O bond distances, with 1.70 and 1.71 Å for Se1 and Se2, respectively, are in agreement with the expected bond lengths.[42,43] Similar to α-$Th(SeO_3)_2$, both Se sites are coordinated by three O atoms, forming trigonal-pyramidal polyhedra. The lone pairs of Se2 atoms are oriented in the negative *c* direction; however, such a distinct behavior cannot be observed for Se1 atoms owing to a more cluttered distribution of their lone pairs. Similar to α-$Th(SeO_3)_2$, the SeO_3 polyhedra in β-$Th(SeO_3)_2$ also function as a linkage to bridge the Th chains to yield a 3D framework. The $Se1O_3$ polyhedra connect three different Th chains by sharing all three corners, whereas $Se2O_3$ polyhedra share an edge with a ThO_8 polyhedron from one chain and a corner with another ThO_8 polyhedron from a different chain (Figure 1d).

Comparison of α-$Th(SeO_3)_2$ and β-$Th(SeO_3)_2$. Both 3D framework polymorphs are built from the edge-sharing ThO_8 polyhedra, forming chains parallel to the [100] direction, which are further connected by SeO_3 trigonal pyramids. The calculated densities for both polymorphs are rather similar (5.885 and 6.072 g/cm^3 for α- and β-$Th(SeO_3)_2$, respectively). The symmetry of the α-polymorph, monoclinic, is lower compared to that of the orthorhombic β-polymorph. Using empirical parameters according to Brese and O'Keefee,[24] the bond valence calculations give BVSs for α-$Th(SeO_3)_2$ of 4.16 vu (valence units) for Th, 4.04 vu for Se1, and 4.06 vu for Se2. For β-$Th(SeO_3)_2$, bond valence calculations for Th, Se1, and Se2 yield 4.00 vu for all three elements. These values fit very well to the expected ones for Th^{IV} and Se^{IV}.

A major difference between these two structures is the interior of the apparently empty voids between adjacent ThO_8 polyhedral chains, where the lone pairs of selenite groups (SeO_3^{2-}) are present. Figure 2 shows the channels accommodated with the selenite polyhedra. For the α-polymorph, the lone pairs of both Se1 and Se2 sites are oriented vertically to the chain direction. For the β-polymorph, however, these lone pairs are directed parallel and vertical to the chain directions for Se1 and Se2, respectively. The second difference is the coordinating behavior of the SeO_3^{2-} groups. One can see that the distance between the upmost O atoms of neighboring ThO_8 polyhedra along the Th chain direction is larger for the β-polymorph. The distance is 2.707 Å for the α-polymorph and 3.612 Å for the β-polymorph, respectively, which is too large for the SeO_3^{2-} group to corner-share these O sites in the β-polymorph.

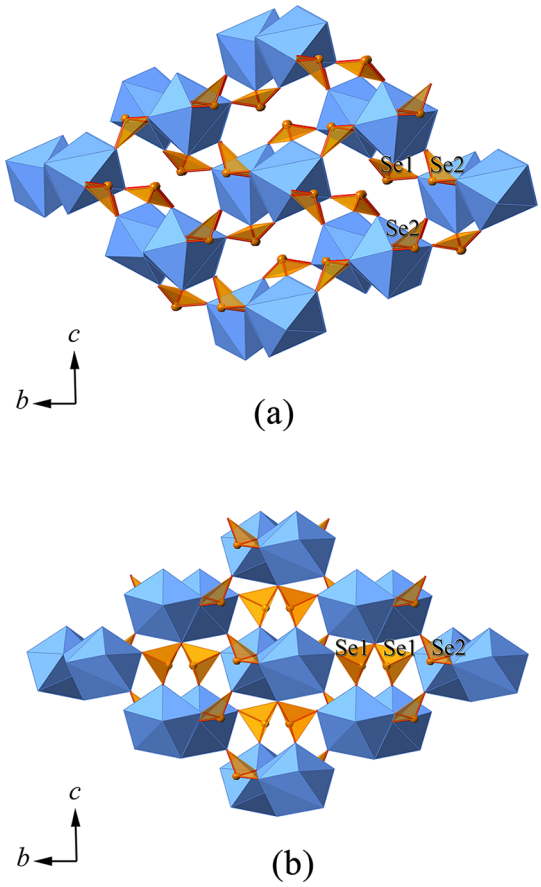

Figure 2. Orientations of lone pairs of SeO_3^{2-} in (a) α-$Th(SeO_3)_2$ and (b) β-$Th(SeO_3)_2$, respectively.

$Th(Se_2O_5)_2$. Using the low-temperature flux method, another new thorium selenite structure was found with the formula $Th(Se_2O_5)_2$, which is shown in Figure 3. The symmetry is orthorhombic with space group *Pbca*. The average Th−O bond length is 2.404 Å. The average Se−O bond length of 1.706 Å fits well to that of other reported selenite groups.[42,43] Shape-measure calculations indicate disordered trigonal dodecahedral geometry for Th atoms. Each SeO_3^{2-} trigonal pyramid shares two corners with two Th polyhedra and the third one with another selenite polyhedron to yield a $Se_2O_5^{2-}$ dimer. The ThO_8 polyhedra are corner-linked to $Se_2O_5^{2-}$ dimers, thus completing the 3D framework. The

DOI: 10.1021/acs.inorgchem.5b00133
Inorg. Chem. 2015, 54, 3022−3030

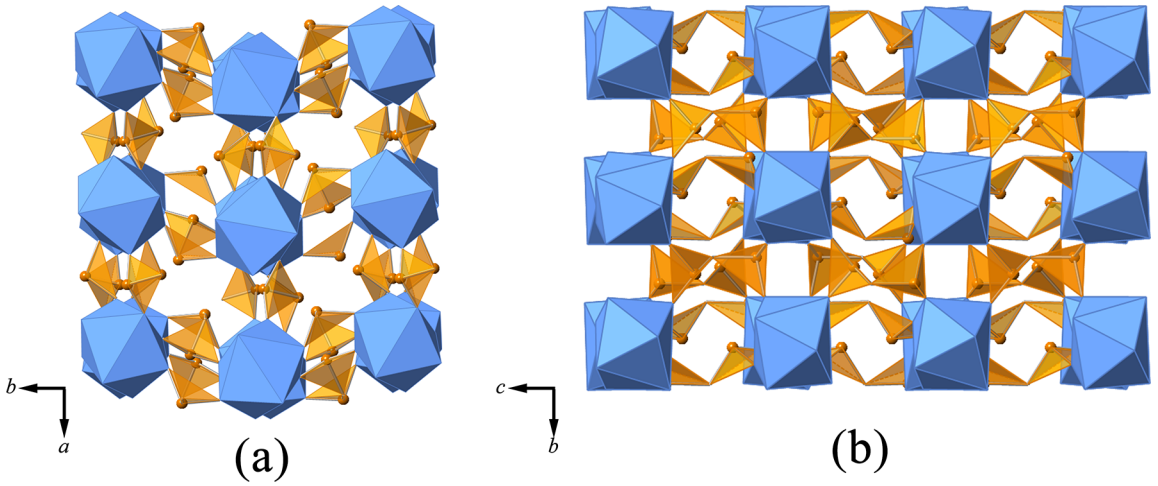

Figure 3. View of the structure of $Th(Se_2O_5)_2$ along the (a) [001] and (b) [100] directions, respectively, demonstrating the connection of ThO_8 polyhedra and $Se_2O_5^{2-}$ dimers.

positions where the O atoms are bonded to two Se atoms each lie within a plane parallel to (001) (Figure 3b). This is the reason why the *c* parameter is the largest because the ThO_8 polyhedra are connected directly by $Se_2O_5^{2-}$ dimers.

$Th_3O_2(OH)_2(SeO_4)_3$. Using hydrothermal acidic conditions, a new thorium selenate was found with the formula $Th_3O_2(OH)_2(SeO_4)_3$. It is interesting that $Th_3O_2(OH)_2(SeO_4)_3$ is similar to tetravalent uranium and cerium hydroxosulfate ($U_6O_4(OH)_4(SO_4)_6$[45] and $Ce_6O_4(OH)_4(SO_4)_6$,[46] respectively). The 3D framework structure adopts a tetragonal system with space group *I*4/*m*, consisting of $[Th_6(\mu_3\text{-}O)_4(\mu_3\text{-}OH)_4]^{12+}$ clusters put together by six Th^{IV} atoms. As shown in Figure 4, these six Th atoms form a nearly regular octahedron, with Th−Th distances ranging from 3.9354(6) to 3.9735(6) Å. The eight faces of the resulting octahedron bridged by either μ_3-O or μ_3-OH groups. In terms of charge balance, here, μ_3-O and μ_3-OH have to be present in equal numbers. Because of the low X-ray scattering efficiency and high residual peaks surrounding the heavy atoms (Th), the H positions were not determined with single-crystal diffraction measurement. Besides, the vibrational frequencies at around 3000 cm^{-1} also show evidence of OH groups (see the Raman Spectral Analysis section). The existence of the protonated μ_3-OH groups within the structure also agrees with the lowest-energy configuration obtained by DFT calculations on the hexameric Th cores.[47] The basic structural feature that fundamentally distinguishes μ_3-OH from μ_3-O sites is a difference in the Th−OH and Th−O bond distances. For instance, the values of the Th−μ_3-OH and Th−μ_3-O bonds in hexanuclear Th-based chloroacetate are 2.486−2.514 and 2.291−2.315 Å, respectively.[48] However, because of the highly symmetric crystal system, the observed difference for Th−μ_3O-(H) bond distances in $Th_6O_4(OH)_4(SeO_4)_6$, from 2.426(11) to 2.448(12) Å, is negligible. The indistinguishable Th−O/OH phenomenon is also reported in several other hexanuclear Th compounds with μ_3O/OH bridging.[48,49] Each Th atom achieves 8-fold coordination by the attachment of four O atoms from μ_3-O/OH and four O atoms from four SeO_4^{2-} groups. The shape-measure calculations resulted in approximately square-antiprismatic geometry for both Th sites. Inside the clusters, the $Th1O_8$ square antiprism shares corners with four separate SeO_4 tetrahedra, two of which are Se1 and the other two are Se2, whereas, $Th2O_8$ are exclusively connected

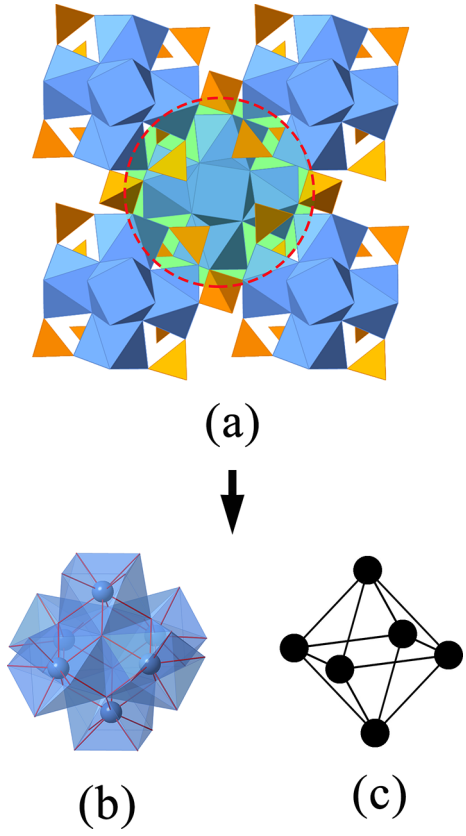

Figure 4. (a) View of the 3D structure $Th_3O_2(OH)_2(SeO_4)_3$. (b) Hexanuclear cluster $[Th_6(\mu_3\text{-}O)_4(\mu_3\text{-}OH)_4]^{12+}$. (c) Schematic representation of the corresponding octahedron composed of the six Th ions.

with four Se1 tetrahedra. The Se1 tetrahedra exhibit an average bond length of 1.625 Å and bond angles ranging from 108.2(6)° to 112.7(1)°. They are within the expected range of selenate ions because they form an almost ideal tetrahedron with an average bond angle of 109.5°. Se2 tetrahedra with an average bond distance of 1.639 Å and angles in the range of 107.3(3)−113.8(7)° are also in compliance with the expected values. The Se1 tetrahedra connect three different $[Th_6(\mu_3\text{-}O)_4(\mu_3\text{-}OH)_4]^{12+}$ clusters by corner sharing with two Th

DOI: 10.1021/acs.inorgchem.5b00133
Inorg. Chem. 2015, 54, 3022−3030

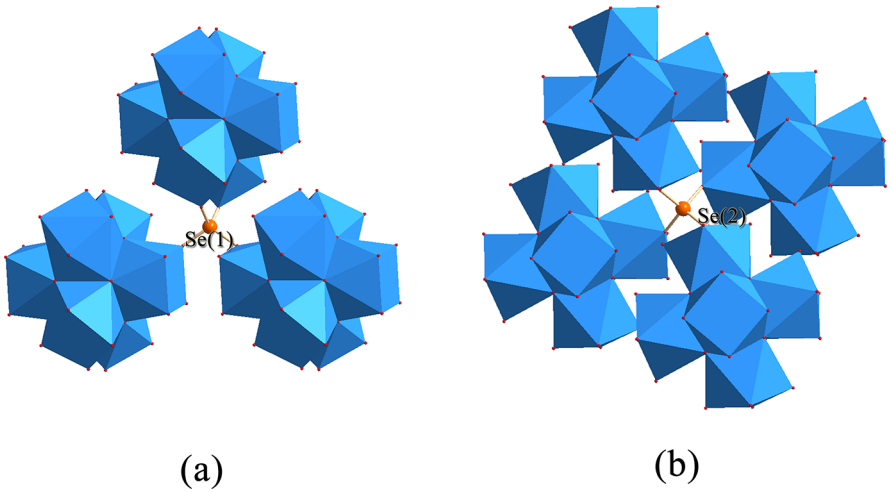

Figure 5. (a) Representation of the linkage of Se1 in the structure of $Th_3O_2(OH)_2(SeO_4)_3$. (b) Representation of the linkage of Se2 in the structure of $Th_3O_2(OH)_2(SeO_4)_3$.

polyhedra from one cluster and two Th polyhedra from two other different clusters (see Figure 5a). Compared to the Se1 tetrahedra, the Se2 tetrahedra share all of their four O vertexes connecting four separate $[Th_6(\mu_3\text{-}O)4(\mu_3\text{-}OH)_4]^{12+}$ clusters (see Figure 5b).

In a comparison of already isolated hexanuclear Th clusters,[48,50,51] no incorporated water was found in the crystal structure of $Th_3O_2(OH)_2(SeO_4)_3$. The fact that similar Pu clusters $[Pu_6(OH)_4O_4]^{12+}$ have been found recently underlines the possibility for using such structures to understand the hydrolysis trends in actinide chemistry.[52]

Raman Spectral Analysis. The ideal SeO_3^{2-} trigonal pyramid has a C_{3v} symmetry consisting of four vibrational frequencies: two nondegenerate v_1 and v_2 modes and two other doubly degenerate v_3 and v_4 modes.[53,54] For each $Th(SeO_3)_2$ polymorph, there are totally 108 normal vibrational modes ($27A_g + 27A_u + 27B_g + 27B_u$ and $27A_1 + 27A_2 + 27B_1 + 27B_2$ for α and β polymorphs, respectively) predicted by the factor group analysis, with some of them being acoustic modes.[55] Figure 6 shows the Raman spectra for both the α and β polymorphs of $Th(SeO_3)_2$ in the range 100−1000 cm^{-1}. The most intense peak, around 855 cm^{-1} in both cases, is expected to be assigned to the symmetric stretching vibration v_1. This position is slightly shifted from 858(1) cm^{-1} for α to 854(1) cm^{-1} for β and well consistent with that determined for a series of alkali selenites by Cody and Mička.[56,57] The asymmetric stretching vibration v_3, on the other hand, behaves quite differently in both polymorphs. For the α polymorph, there are five obvious peaks at approximately 659, 682, 701, 722, and 749 cm^{-1} located in the v_3 vibrational range, whereas for the β polymorph, only two broad bands of strong intensity [692(1) and 740(1) cm^{-1}] are observed for this mode. The difference in the bending vibration v_2 is tiny; both consist of peaks at similar wavenumbers occurring from 450 to 515 cm^{-1}. A comparison may be made with the vibrational spectra of mineral mandarinoite, in which the v_2 modes are located between 449 and 461 cm^{-1}.[58] The v_4 bending mode again shows a big difference. The α polymorph shows a clear peak at 402(1) cm^{-1}, while there is no corresponding peak detected for the β polymorph. Another weak peak at around 363 cm^{-1} may also be attributed to v_4 for the α polymorph. The vibrations for both spectra in the range 100−330 cm^{-1} are mainly due to the coupling modes among O−Th−O bends and lattice vibrations.[59,60]

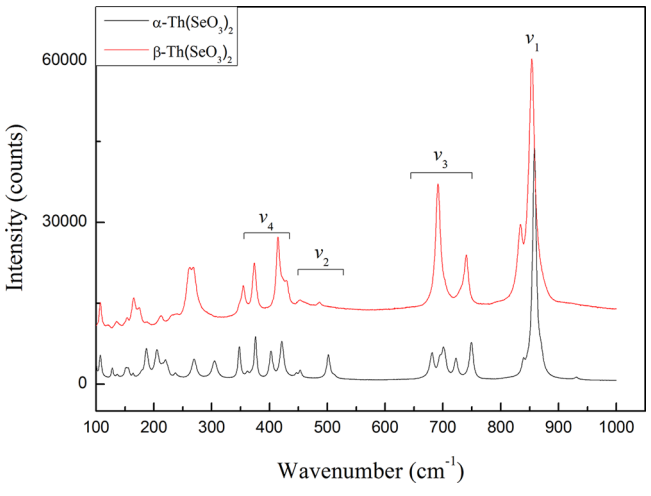

Figure 6. Comparison of Raman shifts for α- and β-$Th(SeO_3)_2$.

From Figure 7, the observed Raman shifts from 300 to 1000 cm^{-1} for $Th(Se_2O_5)_2$ are quite similar to those of $Cu(Se_2O_5)$, a compound for which the vibrational properties have been discussed by Choi et al. by comparing the polarized Raman spectra at different temperatures.[61] This clearly identifies the presence of diselenite units in the compound of $Th(Se_2O_5)_2$. Similar to $Cu(Se_2O_5)$, because of the existence of a high number of crystallographically distinct Se sites in the asymmetrical unit of $Th(Se_2O_5)_2$, more vibrational bands in the stretching region [such as 769(1) and 788(1) cm^{-1}] are detected.

The Raman spectrum shown in Figure 7 for the $Th_3O_2(OH)_2(SeO_4)_3$ structure was recorded in the range 100−3000 cm^{-1}. For the SeO_4^{2-} tetrahedral group, the structural appearance results in four normal modes that are all Raman-active. These modes are the symmetric stretch v_1, the asymmetric stretch v_3, and two bending modes v_2 and v_4. For free SeO_4^{2-} ions in aqueous solution, these frequencies are distributed at 833 (v_1), 335 (v_2), 875 (v_3), and 432 cm^{-1} (v_4), respectively.[62] Within solid-state compounds, however, these modes are expected to shift because of mutual interactions and crystal-field effects.[63] The corresponding values are described

DOI: 10.1021/acs.inorgchem.5b00133
Inorg. Chem. 2015, 54, 3022−3030

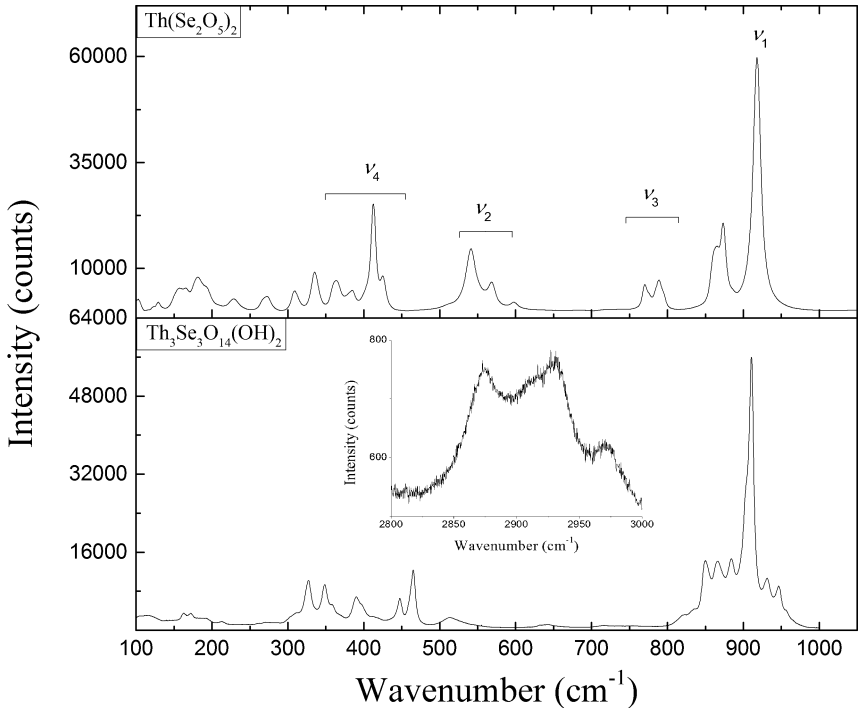

Figure 7. Raman shifts in the compounds of $Th(Se_2O_5)_2$ and $Th_3O_2(OH)_2(SeO_4)_3$, respectively.

by Socrates to be 750−830 cm^{-1} for v_1, 300−370 cm^{-1} for v_2, 830−935 cm^{-1} for v_3, and 350−450 cm^{-1} for v_4.[64] The v_1 peak is said to be the most intense, followed by v_3 and subsequently by the bending modes. In $Th_3O_2(OH)_2(SeO_4)_3$, the spectrum can be coarsely divided into three different parts. The first part is a low-frequency part within the range of 100−250 cm^{-1}, and it can be assigned to lattice modes. The midfrequency range of 300−1000 cm^{-1} is mostly associated with the internal motions within the SeO_4^{2-} tetrahedra. The third part around 3000 cm^{-1} belongs to the high-frequency part showing the vibrational behavior of the hydroxyl units. As can be seen in Figure 7, the Raman spectrum in the lower-frequency range (from 100 to 250 cm^{-1}) has a weak signal-to-noise ratio, and therefore no direct information can be taken from this range. The midfrequency range contains a lot of strong bands, and these can partly be assigned to distinct modes. The bands located at 328(1) and 349(1) cm^{-1} might be assigned to the v_2 bending mode. The v_4 bending mode is most likely resembles the 465(1) cm^{-1} band. The weak band at 515(1) cm^{-1} can possibly be assigned to Th−O stretching. Knope et al. investigated similar clusters containing octanuclear cores, and they found the Th−O stretch to be at 528 cm^{-1}.[22] The strong peak at 910(1) cm^{-1} is associated with the v_1 stretch of the selenate ion. The two bands at 932(1) and 947(1) cm^{-1} might correspond to the v_3 mode of the selenate group. In general, the two assigned stretching modes appear to be at slightly higher wavenumbers than those for free selenate ions. Owing to the low Raman scattering intensity properties of the OH^- group, bands in the high-frequency range just below 3000 cm^{-1} are low in the signal-to-noise ratio. These shifts are comparable to the spectra of guilleminite (observed also at around 3000 cm^{-1}).[65]

4. CONCLUSION

The compounds discussed here, containing SeO_4^{2-}, SeO_3^{2-}, and $Se_2O_5^{2-}$ units, display an outstanding diversity regarding the coordination geometry of Se cations. α- and β-$Th(SeO_3)_2$ are based on similar structural skeletons but differ mainly with respect to the orientation of the SeO_3^{2-} trigonal pyramids. It is clear that, because of a lack of O connections between neighboring ThO_8 polyhedra in $Th(Se_2O_5)_2$, all ThO_8 polyhedra are thoroughly isolated from each other by neighboring $Se_2O_5^{2-}$ units. $Th_3O_2(OH)_2(SeO_4)_3$ is by far the first inorganic compound containing hexanuclear Th clusters. The Raman spectra show typical vibrational modes for selenites and selenates in the studied phases with local features with respect to their symmetry. These four new Th−Se compounds, together with another previously published $Th(SeO_3)(SeO_4)$ compound,[21] become a cornerstone for studying other actinide complexation, such as Np^{IV} and Pu^{IV}, in O−Se systems. It is clear that the introduction of countercations, such as alkali or alkaline-earth metals, will generate more chemically and structurally complex phases in the studied systems.

■ ASSOCIATED CONTENT

Supporting Information

EDS analysis, atomic ratios, and CIF files. This material is available free of charge via the Internet at http://pubs.acs.org.

■ AUTHOR INFORMATION

Corresponding Author

*E-mail: e.alekseev@fz-juelich.de.

Notes

The authors declare no competing financial interest.

■ ACKNOWLEDGMENTS

The authors are grateful to Dr. Martina Klinkenberg (IEK-6, Forschungszentrum Jülich GmbH) for her kind help in electron microscopy and energy-dispersive X-ray experiments. We are grateful to the Helmholtz Association for funding within Grant VH-NG-815. E.V.S. is grateful to the Centre of Collective Use

DOI: 10.1021/acs.inorgchem.5b00133
Inorg. Chem. 2015, 54, 3022−3030

"New materials and energy saving technologies" (Project RFMEFI59414X0005).

REFERENCES

(1) Krivovichev, S. V.; Kahlenberg, V. *J. Alloys Compd.* **2005**, *389*, 55−60.
(2) Burns, P. C.; Miller, M. L.; Ewing, R. C. *Can. Mineral.* **1996**, *34*, 845−845.
(3) Dacheux, N.; Thomas, A.; Chassigneux, B.; Pichot, E.; Brandel, V.; Genet, M. *Study of $Th_4(PO_4)_4P_2O_7$ and Solid Solutions with U(IV), Np(IV) and Pu(IV): Synthesis, Characterization, Sintering and Leaching Tests*; MRS Proceedings; Cambridge Univ Press: Cambridge, U.K., 1999; p 85.
(4) Wilson, R. E.; Skanthakumar, S.; Burns, P. C.; Soderholm, L. *Angew. Chem.* **2007**, *119*, 8189−8191.
(5) Wang, G.; Zhang, L.; Lin, Z.; Wang, G. *J. Alloys Compd.* **2010**, *489*, 293−296.
(6) Wang, S.; Yu, P.; Purse, B. A.; Orta, M. J.; Diwu, J.; Casey, W. H.; Phillips, B. L.; Alekseev, E. V.; Depmeier, W.; Hobbs, D. T.; Albrecht-Schmitt, T. E. *Adv. Funct. Mater.* **2012**, *22*, 2241−2250.
(7) Yu, P.; Wang, S.; Alekseev, E. V.; Depmeier, W.; Hobbs, D. T.; Albrecht-Schmitt, T. E.; Phillips, B. L.; Casey, W. H. *Angew. Chem., Int. Ed.* **2010**, *49*, 5975−5977.
(8) Fanghänel, T.; Neck, V. *Pure Appl. Chem.* **2002**, *74*, 1895−1907.
(9) Neck, V.; Kim, J. *Radiochim. Acta* **2001**, *89*, 1−16.
(10) Knope, K. E.; Wilson, R. E.; Vasiliu, M.; Dixon, D. A.; Soderholm, L. *Inorg. Chem.* **2011**, *50*, 9696−9704.
(11) Woidy, P.; Kraus, F. *Z. Anorg. Allg. Chem.* **2014**, *640*, 1547−1550.
(12) Kersting, A.; Efurd, D.; Finnegan, D.; Rokop, D.; Smith, D.; Thompson, J. *Nature* **1999**, *397*, 56−59.
(13) Novikov, A. P.; Kalmykov, S. N.; Utsunomiya, S.; Ewing, R. C.; Horreard, F.; Merkulov, A.; Clark, S. B.; Tkachev, V. V.; Myasoedov, B. F. *Science* **2006**, *314*, 638−641.
(14) Barney, G. S.; Wood, B. J. *Identification of key radionuclides in a nuclear waste repository in basalt*; Rockwell Hanford Operations, Rockwell International Corp.: Richland, WA, 1980.
(15) Almond, P. M.; Albrecht-Schmitt, T. E. *Inorg. Chem.* **2002**, *41*, 1177−1183.
(16) Almond, P. M.; Albrecht-Schmitt, T. E. *Inorg. Chem.* **2003**, *42*, 5693−5698.
(17) Kong, F.; Huang, S.-P.; Sun, Z.-M.; Mao, J.-G.; Cheng, W.-D. *J. Am. Chem. Soc.* **2006**, *128*, 7750−7751.
(18) Alekseev, E. V.; Krivovichev, S. V.; Depmeier, W. *Angew. Chem., Int. Ed.* **2008**, *47*, 549−551.
(19) Krivovichev, S. V.; Kahlenberg, V.; Kaindl, R.; Mersdorf, E.; Tananaev, I. G.; Myasoedov, B. F. *Angew. Chem.* **2005**, *117*, 1158−1160.
(20) Mellor, J. W. *A Comprehensive Treatise of Inorganic and Theoretical Chemistry*; Longmans, Green, and Co.: London, 1948; Vol. *10*, p 833.
(21) Sullens, T. A.; Almond, P. M.; Byrd, J. A.; Beitz, J. V.; Bray, T. H.; Albrecht-Schmitt, T. E. *J. Solid State Chem.* **2006**, *179*, 1192−1201.
(22) Knope, K. E.; Vasiliu, M.; Dixon, D. A.; Soderholm, L. *Inorg. Chem.* **2012**, *51*, 4239−4249.
(23) Sheldrick, G. *Acta Crystallogr., Sect. A: Found. Crystallogr.* **2008**, *64*, 112−122.
(24) Brese, N. E.; O'Keeffe, M. *Acta Crystallogr., Sect. B: Struct. Sci.* **1991**, *47*, 192−197.
(25) Wang, S.; Alekseev, E. V.; Depmeier, W.; Albrecht-Schmitt, T. E. *Chem. Commun. (Cambridge, U. K.)* **2010**, *46*, 3955−3957.
(26) Wang, S.; Alekseev, E. V.; Depmeier, W.; Albrecht-Schmitt, T. E. *Chem. Commun. (Cambridge, U. K.)* **2011**, *47*, 10874−10885.
(27) Wang, S.; Alekseev, E. V.; Depmeier, W.; Albrecht-Schmitt, T. E. *Inorg. Chem.* **2011**, *50*, 2079−2081.
(28) Wang, S.; Alekseev, E. V.; Depmeier, W.; Albrecht-Schmitt, T. E. *Inorg. Chem.* **2011**, *50*, 4692−4694.
(29) Wang, S.; Alekseev, E. V.; Depmeier, W.; Albrecht-Schmitt, T. E. *Inorg. Chem.* **2012**, *51*, 7−9.
(30) Wang, S.; Alekseev, E. V.; Diwu, J.; Casey, W. H.; Phillips, B. L.; Depmeier, W.; Albrecht-Schmitt, T. E. *Angew. Chem., Int. Ed.* **2010**, *49*, 1057−1060.
(31) Knope, K. E.; Soderholm, L. *Chem. Rev.* **2012**, 944−994.
(32) Delage, C.; Carpy, A.; H'Naifi, A.; Goursolle, M. *Acta Crystallogr., Sect. C* **1986**, *42*, 1475−1477.
(33) Meier, S. F.; Weber, F. A.; Gläser, R. J.; Schleid, T. *Z. Anorg. Allg. Chem.* **2001**, *627*, 2448−2450.
(34) López, M. L.; Veiga, M. L.; Jerez, A.; Pico, C. *J. Less Common Met.* **1991**, *175*, 235−241.
(35) Krishnan, K.; Mudher, K. D. S.; Venugopal, V. *J. Alloys Compd.* **2000**, *307*, 114−118.
(36) Bray, T. H.; Skanthakumar, S.; Soderholm, L.; Sykora, R. E.; Haire, R. G.; Albrecht-Schmitt, T. E. *J. Solid State Chem.* **2008**, *181*, 493−498.
(37) Xiao, B.; Dellen, J.; Schlenz, H.; Bosbach, D.; Suleimanov, E. V.; Alekseev, E. V. *Cryst. Growth Des.* **2014**, *14*, 2677−2684.
(38) Xiao, B.; Gesing, T. M.; Kegler, P.; Modolo, G.; Bosbach, D.; Schlenz, H.; Suleimanov, E. V.; Alekseev, E. V. *Inorg. Chem.* **2014**, *53*, 3088−3098.
(39) Xu, J.; Radkov, E.; Ziegler, M.; Raymond, K. N. *Inorg. Chem.* **2000**, *39*, 4156−4164.
(40) Bang Jin, G.; Soderholm, L. *J. Solid State Chem.* **2011**, *184*, 337−342.
(41) Sullens, T. A.; Albrecht-Schmitt, T. E. *Inorg. Chem.* **2005**, *44*, 2282−2286.
(42) Almond, P. M.; Albrecht-Schmitt, T. E. *Inorg. Chem.* **2002**, *41*, 1177−1183.
(43) Almond, P. M.; Peper, S. M.; Bakker, E.; Albrecht-Schmitt, T. E. *J. Solid State Chem.* **2002**, *168*, 358−366.
(44) Almond, P. M.; Peper, S. M.; Bakker, E.; Albrecht-Schmitt, T. E. *J. Solid State Chem.* **2002**, *171*, 455.
(45) Lundgren, G. *Ark. Kemi* **1952**, *5*, 349−363.
(46) Lundgren, G. *Ark. Kemi* **1957**, *10*, 183−197.
(47) Vasiliu, M.; Knope, K. E.; Soderholm, L.; Dixon, D. A. *J. Phys. Chem. A* **2012**, *116*, 6917−6926.
(48) Knope, K. E.; Wilson, R. E.; Vasiliu, M.; Dixon, D. A.; Soderholm, L. *Inorg. Chem.* **2011**, *50*, 9696−9704.
(49) Falaise, C.; Charles, J.-S.; Volkringer, C.; Loiseau, T. *Inorg. Chem.* **2015**, DOI: 10.1021/ic502725y.
(50) Hennig, C.; Takao, S.; Takao, K.; Weiss, S.; Kraus, W.; Emmerling, F.; Scheinost, A. C. *Dalton Trans.* **2012**, *41*, 12818−12823.
(51) Takao, S.; Takao, K.; Kraus, W.; Emmerling, F.; Scheinost, A. C.; Bernhard, G.; Hennig, C. *Eur. J. Inorg. Chem.* **2009**, *2009*, 4771−4775.
(52) Knope, K. E.; Soderholm, L. *Inorg. Chem.* **2013**, *52*, 6770−6772.
(53) Dussack, L. L.; Harrison, W. T. A.; Jacobson, A. J. *Mater. Res. Bull.* **1996**, *31*, 249−255.
(54) Ratheesh, R.; Suresh, G.; Bushiri, M. J.; Nayar, V. U. *Spectrochim. Acta, Part A* **1995**, *51*, 1509−1515.
(55) Rousseau, D. L.; Bauman, R. P.; Porto, S. P. S. *J. Raman Spectrosc.* **1981**, *10*, 253−290.
(56) Cody, C. A.; Levitt, R. C.; Viswanath, R. S.; Miller, P. J. *J. Solid State Chem.* **1978**, *26*, 281−291.
(57) Mička, Z.; Daněk, M.; Loub, J.; Strauch, B.; Podlahová, J.; Hašek, J. i. *J. Solid State Chem.* **1988**, *77*, 306−315.
(58) Frost, R. L.; Keeffe, E. C. *J. Raman Spectrosc.* **2009**, *40*, 42−45.
(59) Frost, R. L.; Keeffe, E. C. *J. Raman Spectrosc.* **2009**, *40*, 128−132.
(60) Khandelwal, B. L.; Verma, V. P. *J. Inorg. Nucl. Chem.* **1976**, *38*, 763−769.
(61) Choi, K. Y.; Lemmens, P.; Berger, H. *Phys. Rev. B* **2011**, *83*, 174413−174413.
(62) Nakamoto, K. *Infrared and Raman spectra of inorganic and coordination compounds*; Wiley Online Library: New York, 1978.
(63) Jin, G. B.; Skanthakumar, S.; Soderholm, L. *Inorg. Chem.* **2012**, *51*, 3220−3230.
(64) Socrates, G. *Infrared and Raman characteristic group frequencies: tables and charts*; Wiley: Chichester, U.K., 2001; Vol. *245*.

DOI: 10.1021/acs.inorgchem.5b00133
Inorg. Chem. 2015, 54, 3022−3030

(65) Frost, R. L.; Čejka, J.; Dickfos, M. J. *J. Raman Spectrosc.* **2009**, *40*, 355−359.

DOI: 10.1021/acs.inorgchem.5b00133
Inorg. Chem. 2015, 54, 3022−3030